



Contents lists available at ScienceDirect

Quaternary International

journal homepage: www.elsevier.com/locate/quaint

Summer atmospheric bridging between Europe and East Asia: Influences on drought and wetness on the Tibetan Plateau

Xiuhua Zhu^{a,*}, Oliver Bothe^b, Klaus Fraedrich^b

^a Max Planck Institute for Meteorology, KlimaCampus, Bundesstr. 53, D-20146 Hamburg, Germany

^b Meteorological Institute, KlimaCampus, University of Hamburg, Germany

ARTICLE INFO

Article history:

Available online xxx

ABSTRACT

Based on the ERA-40 reanalysis data, dryness and wetness over the Tibetan Plateau are categorized according to the monthly standardized precipitation index. The atmospheric features associated with severe and extreme dryness and wetness reveal two cross-Eurasia wave trains: the Scandinavia-East Asia wave train and the Mediterranean-East Asia wave train. Severe and extreme dryness is associated with an anomalous cyclone over south and southeast Asia, which directs the moisture supply from the Arabian Sea, the Bay of Bengal, and the South China Sea directly eastward towards the western Pacific, thus bypassing the Tibetan Plateau. This cyclone anomaly constitutes part of the Scandinavia-East Asia wave train, which is sustained by the divergence and convergence of the anomalous transient eddy heat transport associated with a more southwest-northeast oriented North Atlantic storm track and a northward shift of the polar front jet in the North Atlantic.

In contrast, severe and extreme wetness over the Tibetan Plateau is associated with a more zonally elongated North Atlantic storm track; wave trains excited from there have a high probability to reach the Mediterranean region and to propagate eastward following the subtropical westerly jet. This Mediterranean-East Asia wave train generates anticyclonic anomalies around the Tibetan Plateau and East China, which bring more moisture supply from the Arabian Sea, the South China Sea, and the western Pacific towards the Tibetan Plateau and enhance the moisture convergence there. This paper demonstrates how atmospheric bridging processes affect regional climate variability under present day climatic conditions, which are also relevant for understanding past climates.

© 2010 Elsevier Ltd and INQUA. All rights reserved.

1. Introduction

The Tibetan Plateau covers an area of half the size of the United States which, with an average elevation of about 4 km, acts as a mechanical barrier and an elevated heat source affecting the climate from geological to intra- and inter-annual time scales. It has been revealed (An et al., 2001) that the uplift of the Tibetan Plateau plays a fundamental role in the development of the Asian monsoon system. The Tibetan Plateau provides water sources for Asia's major rivers (Fekete et al., 1999, 2000), affecting the life of a quarter of the world's population. Thus it is important to investigate the regional water cycle variability and extreme events like severe and extreme drought and wetness.

The Tibetan Plateau is subject to influences of modes associated with the global circulation: (i) on the intra- and inter-annual

timescales, the North Atlantic Oscillation (NAO) has an impact on the temporal and spatial precipitation variability over the eastern part of the Tibetan Plateau (Liu and Yin, 2001); (ii) on decadal to centennial timescales, it has been reported that the North Atlantic multidecadal and the Pacific decadal oscillations may affect Eurasia (Ye, 2000; Gupta et al., 2003; Goswami et al., 2006; d'Orgeville and Peltier, 2007; Zhang and Delworth, 2006, 2007; Feng and Hu, 2008).

The remote influence on the Tibetan Plateau is supported by circumglobal teleconnections (e.g., Branstator, 2002; Yang et al., 2004; Ding and Wang, 2005). Yang et al. (2004) report that the winter and spring NAO may affect the strength and shift of the Middle East jet stream and the associated stationary wave activity flux and higher-frequency eddy activities, which subsequently affect the downstream Asian summer monsoon (ASM) system dominating over the Tibetan Plateau. Ding and Wang (2005) document a cross-Eurasia wave train linking North Atlantic to Eurasia in summer: the strong barotropic instability at the jet exit region in the North Atlantic triggers an anomalous high over western Europe, favoring a Rossby wave train stretching from western Europe to western central Asia.

* Corresponding author. Tel.: +49 40 42838 5072; fax: +49 40 42838 5066.

E-mail addresses: xiuhua.zhu@zmaw.de (X. Zhu), oliver.bothe@zmaw.de (O. Bothe), klaus.fraedrich@zmaw.de (K. Fraedrich).

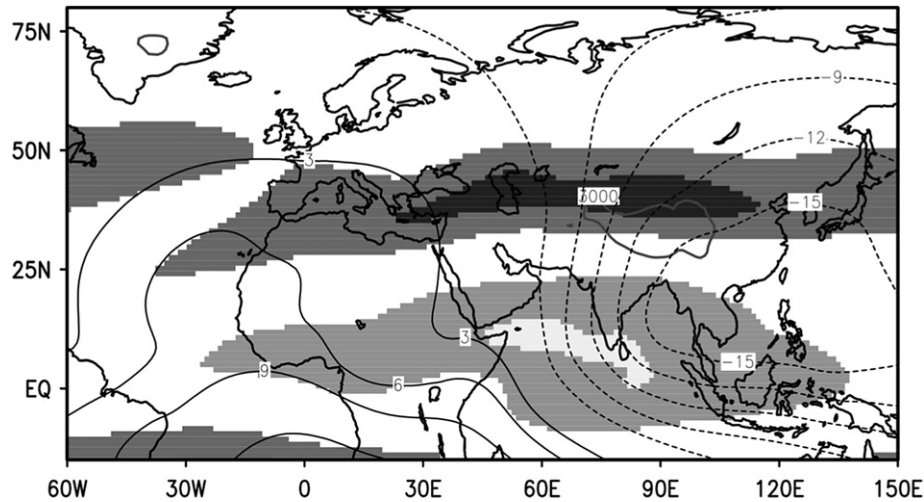


Fig. 1. Climatological summer (JJA) flow setting at 200 hPa: velocity potential (unit: $10^{-6} \text{ m}^2/\text{s}$, contours) and zonal wind (unit: m/s, shaded). Shades from light to dark gray denote -20, -10, 10, and 20. The Tibetan Plateau is highlighted by the 3000 m contour (thick dark gray).

Accompanying this wave train, strong stationary wave energy is transported from western Europe high latitudes to western central Asia, inducing a secondary anomalous high, which further reinforces the instability associated with the easterly jet and affects monsoon precipitation. Similar wave trains bridging Europe and Asia are often supported by waveguides along the mid-latitude and by the subtropical jets (e.g., Hoskins and Ambrizzi, 1993; Ambrizzi et al., 1995; Branstator, 2002; Goswami et al., 2006; Li et al., 2008).

While the Tibetan Plateau is exposed to upstream forcings, signals appearing over the Tibetan Plateau and the ASM region can also generate wave trains influencing East Asia, the western Pacific and further downstream. For example, it has been reported that the Indian summer monsoon is an important component of the ASM, and can generate an upper-level anomalous high to its northwest over west-central Asia thus exciting successive downstream cells along the wave guide through Rossby wave dispersion and influencing the North Pacific and North America (Ding and Wang, 2005). Another example is that anomalous high temperature over the Tibetan Plateau will induce two baroclinic Rossby wave trains, one propagating downstream along the upper-level westerly jet stream

to enhance the circulation near Japan, the other propagating into the South China Sea enhancing the low-level anticyclonic ridge there. Both wave trains deform the western North Pacific subtropical high and enhance moisture convergence towards the East Asia subtropical front (Wang et al., 2008).

This paper focuses on drought and wetness as water cycle extremes over the Tibetan Plateau, which are modulated by atmospheric wave trains. In summer, two types of wave trains emerging from the North Atlantic storm track are responsible for modifying the Tibetan Plateau water supply: the Scandinavia-East Asia wave train via central Asia and the eastern North Atlantic to East Asia wave train via the Mediterranean region. Both are vital for the variability of the water cycle in Asia but have rarely been investigated.

This paper is organized as follows: Section 2 introduces data sources and the climatological settings, and Section 3 presents composite analyses to highlight the Scandinavia-East Asia and the Mediterranean-East Asian wave trains; section 4 presents conclusions and discussions. To classify dryness and wetness over the Tibetan Plateau, the standardized precipitation index (SPI) is derived from monthly precipitation time series based on equal

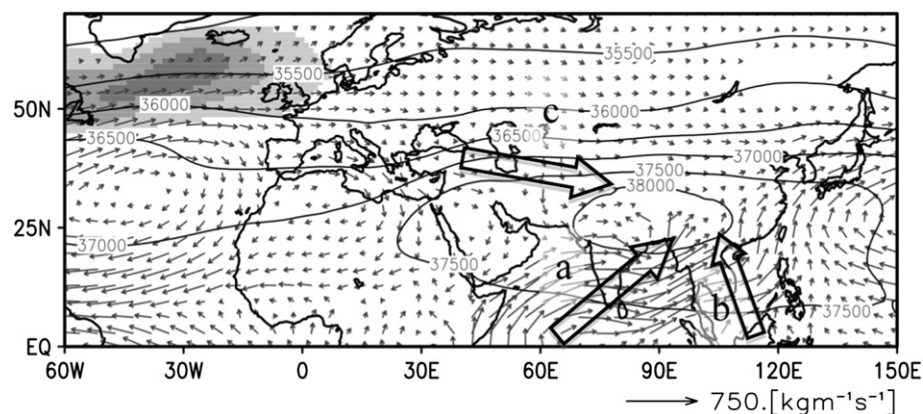


Fig. 2. Climatological summer (JJA) circulation: upper layer mean geopotential height calculated as $0.5 \times (300 + 500) \text{ hPa}$ (unit: m^2/s^2 , contour), vertically integrated moisture supply (unit: $\text{kg}/\text{m}/\text{s}$, vector), and 500 hPa storm track (unit: $10^3 \text{ m}^4/\text{s}^4$, shaded). Shades from light to dark gray denote 900, 1200, and 1500. Moisture vectors magnitudes below 25 $\text{kg}/\text{m}/\text{s}$ are omitted. Big black arrows depict three routes of moisture supply to the Tibetan Plateau: a) from the Arabian Sea and the Bay of Bengal, b) from the South China Sea and the Western Pacific, and c) from the North Atlantic.

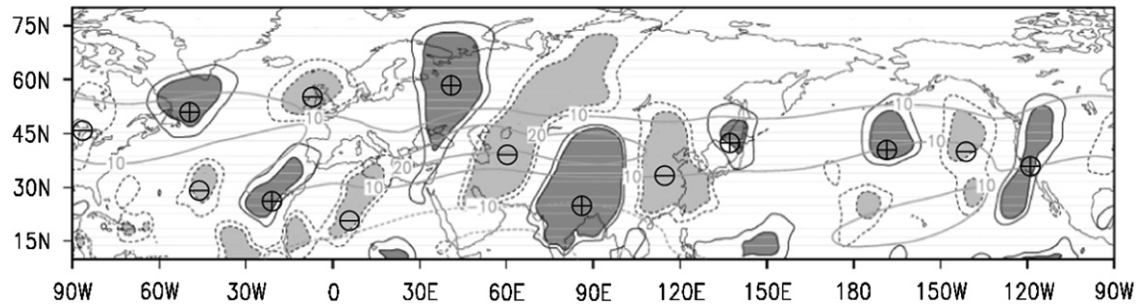


Fig. 3. One-point teleconnection map: spatial distribution of correlation of 200 hPa meridional velocity in July with the time series averaged over the base area over (86°E–96°E, 30–35°N). Contours denote ± 0.2 and ± 0.3 ; dark (light) shading denote values larger (smaller) than (–) 0.3; thick gray lines denote the 200 hPa zonal wind at intervals ± 10 and ± 20 m/s. Teleconnection action centers are highlighted by \oplus and \ominus .

probability transformation (see Bordi and Sutera, 2001, details are given in the Appendix).

2. Tibetan Plateau climatological setting

2.1. Data sources

Precipitation data between 1951 and 2000 is taken from the Vasclimo-climatology (Variability Analysis of Surface Climate Observations, Beck et al., 2005), with 1.0 by 1.0° resolution. Surface and upper air data are obtained from the European Centre for Medium-range Weather Forecast (ECMWF) reanalysis data (ERA-40, Uppala et al., 2005). Based on in situ and remote sensing measurements, the reanalysis data produces physically consistent space-time interpolation of historical observational data and makes it possible to carry out detailed analyses of weather systems. The ECMWF model is run at TL159 horizontal resolution ($1.125 \times 1.125^\circ$) with 60 vertical model levels, covering the period from September 1957 to August 2002. In this paper, analyses focus on the summer season (June, July, and August, if not specified otherwise) from the overlapping period 1958–2000.

2.2. Climatological setting

The Tibetan Plateau is under the influence of the tropical Walker circulation, which is characterized by upper-level divergent flows centred at the tropical western Pacific and convergent flows east to the Tibetan Plateau extending to Africa and the tropical Atlantic (Fig. 1). At the same time, as an elevated heat source (Flohn, 1964, 1968), indicated by the enhanced thickness between two geopotential height

levels (Fig. 2), the Tibetan Plateau is surrounded by an anticyclonic circulation comprising the subtropical westerly jet and the tropical easterly jet in the upper troposphere (Fig. 1).

In summer the Tibetan Plateau is part of the ASM system, which brings along a large amount of moisture from the surrounding oceans (Fig. 2): (a) the Indian summer monsoon transports moisture from the Arabian Sea and from the Bay of Bengal onto the Tibetan Plateau; (b) the southeastern Asian monsoon and the western North Pacific subtropical high carry warm moist air from the South China Sea and the western Pacific towards the Tibetan Plateau. Besides, (c) the mid-latitude westerlies supply the northern parts of the Tibetan Plateau with moisture mostly originated from the North Atlantic.

Wave trains (and storm tracks as wave makers) are part of the circumpolar teleconnections and large scale bridging processes, often appearing along and near the main jet streams. In the hemispheric correlation field of the daily meridional velocity (at 200 hPa) against its average over the area 86–96°E, 30–35°N, the following results are noteworthy (Fig. 3): two wave trains occur crossing Eurasia, one extending southeastward from Scandinavia to the Tibetan Plateau and further continuing to Japan, and the other generated in the eastern subtropical Atlantic extending eastward to the Mediterranean region and north of Africa; a third wave train emerges in the central North Pacific, expanding eastward to North America and the North Atlantic, with a center of action south of Greenland.

3. Eurasian wave train composites

The summer monthly precipitation averaged over the Tibetan Plateau is used to calculate the one-month SPI (SPI-1), which is

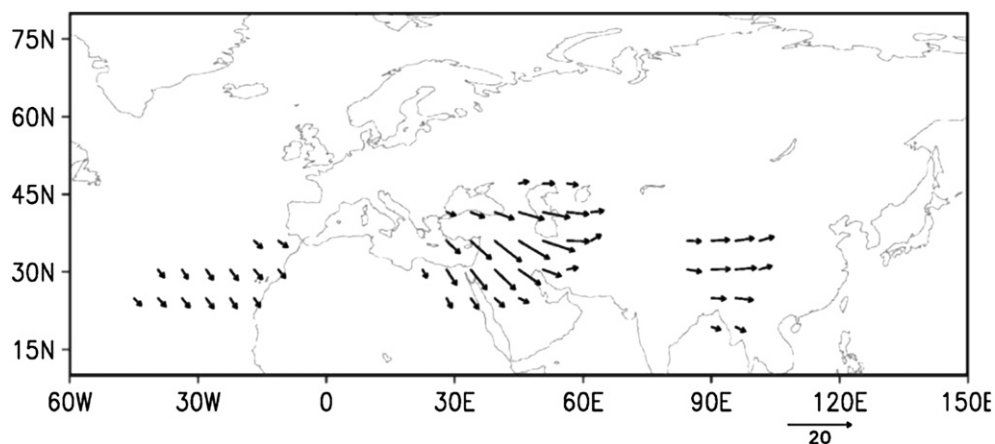


Fig. 4. Stationary Plumb wave fluxes estimated from summer climatological velocity and temperature (unit: m^2/s^2); wave fluxes with magnitude smaller than $3 \text{ m}^2/\text{s}^2$ are not shown.

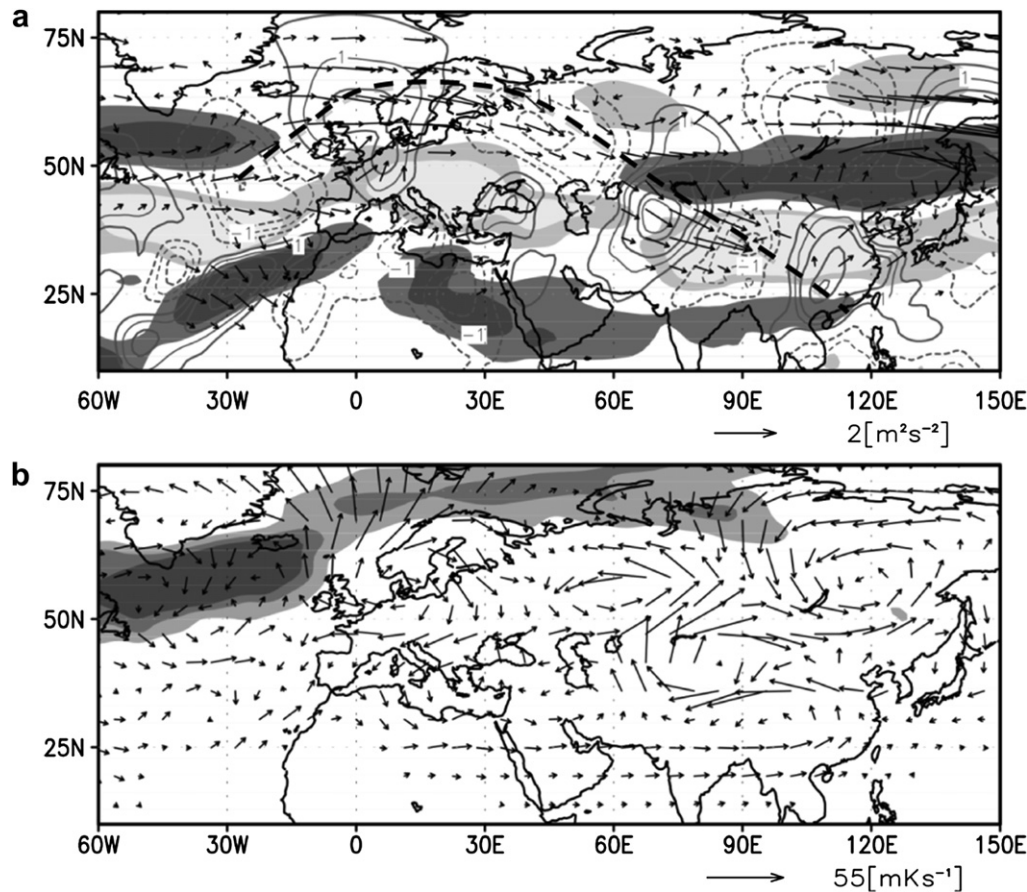


Fig. 5. Composite anomalies for severe and extreme dry cases: a) jet stream (unit: m/s , shaded, from light to dark is $-2, -1, 1$, and 2 ms^{-1}) and meridional velocity at 200 hPa (unit: m/s , contour, positive/negative values denote northward/southward winds), and Plumb's stationary wave flux at 500 hPa (unit: m^2/s^2 , arrows); b) transient eddy heat flux (unit: m^4/s^4 , vector), and storm track at 500 hPa as variance of geopotential height (unit: m^4/s^4 , shaded, from light to dark are 900, 1200, and 1500 m^4/s^4). Thick black dashed line in a) denotes the Scandinavia-East Asia wave train.

taken as a meteorological measure of dryness and wetness. Six cases of severe and extreme drought ($\text{SPI} \leq -1.5$, June 1961, June 1965, June and August of 1972, August 1984, and July 1994) and eleven cases of severe and extreme wetness ($\text{SPI} \geq 1.5$, August of 1958 and 1962, June of 1971, 1973 and 1978, July 1981, June 1984, August 1991, July 1996, August 1998, and June 2000) are considered to form the dry and wet composites respectively. In comparison to wet cases, dry cases occurred less frequently due to an increase of very wet summer months in the late 20th century (1996–2000).

The composite atmospheric dynamic patterns, which are associated with the severe and extreme dry and wet cases, highlight the influences of two stationary wave trains across Eurasia: the Scandinavia-East Asia and the Mediterranean-East Asia wave trains, both of which are associated with transient eddy activities induced by the North Atlantic storm track. It is the feedback between these transient and stationary eddies which forms the atmospheric bridge across Eurasia.

For later ease of comparison, the summer mean stationary wave flux is displayed in Fig. 4. There are three centers of wave activities: near Azores, between the Mediterranean region and the Caspian Sea, and near the Tibetan Plateau. Note that the composite anomalies of the following two wave trains represent only deviations from this climatological mean.

3.1. Scandinavia-East Asia bridge

A remarkable atmospheric feature related to severe and extreme droughts over the Tibetan Plateau is a wave train, depicted by

a series of meridional velocity anomalies with alternate signs (Fig. 5a), emerging from the subpolar North Atlantic and propagating on a 'great circle route' southeastward to the Tibetan Plateau and southeastern China, where the meridional velocity anomalies superimpose on the local changes of the jet system, namely, easterly anomalies in middle China and westerly anomalies in North China and Mongolia and in south and southeast Asia. Consequently, most of the Tibetan Plateau is exposed to anticyclonic anomalies (Fig. 5a, southwesterly/northeasterly anomalies northwest/in the middle of the Tibetan Plateau). Its southern part is influenced by cyclonic anomalies (northeasterly/westerly anomalies in the middle of/south to the Tibetan Plateau) that dominate north India and southeast Asia. The cyclonic anomalies carry the moisture sources from the Arabian Sea, the Bay of Bengal, and the South China Sea more directly eastward towards the western Pacific thus bypassing the Tibetan Plateau (see Fig. 4b from Bothe et al., 2010). This wave train is clearly detectable in the composite stationary wave activity flux anomalies showing the anomalous stationary wave energy flux from Scandinavia to the Tibetan Plateau via central Asia (Fig. 5a).

Origin and persistence of this wave train are associated with the transient eddy activity of the North Atlantic. A more southwest-northeast oriented North-Atlantic storm track (Fig. 5b) shifts the atmospheric polar front jet northward and leads to increased westerlies over the subpolar North Atlantic (Fig. 5a). The anomalous transient eddy heat transport leads to convergence near Iceland and divergence over Scandinavia (Fig. 5b), supporting a stationary cyclone-anticyclone pair in terms of an anomalous

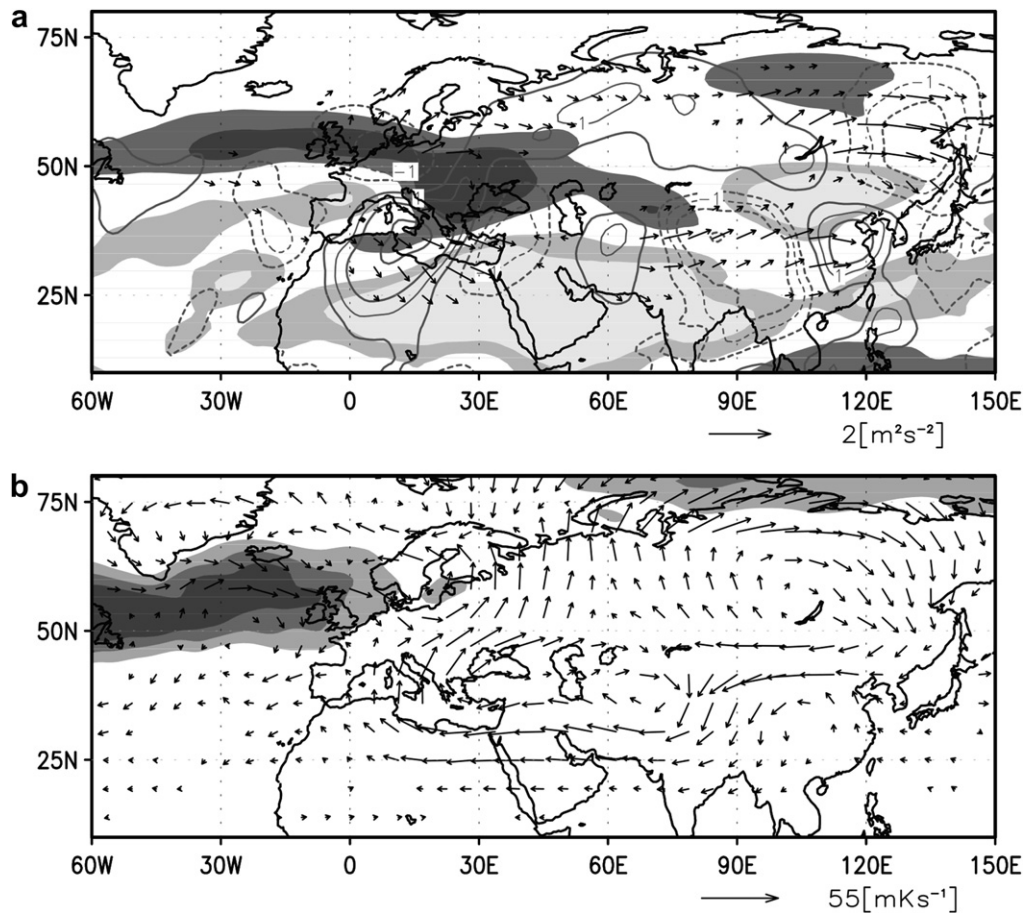


Fig. 6. Composite anomalies for severe and extreme wet cases: a) jet stream (unit: m/s, shaded, from light to dark is -2 , -1 , 1 , and 2 m/s) and meridional velocity at 200 hPa (unit: m/s, contour, positive/negative values denote northward/southward winds), and Plumb's stationary wave flux at 500 hPa (unit: m^2/s^2 , arrows); b) transient eddy heat flux (unit: $\text{m}\cdot\text{K}/\text{s}$, vector), and storm track at 500 hPa as variance of geopotential height (unit: m^4/s^4 , shaded, from light to dark are 900, 1200, and $1500 \text{ m}^4/\text{s}^4$). Thick black dashed line in a) denotes the Mediterranean-East Asia wave train.

geopotential height dipole in the North Atlantic, with the negative center over Iceland and the positive one over Scandinavia (Fig. 5a, northerly/southerly wind anomalies west/east of Iceland and northerly wind anomalies east to Scandinavia). The anomalous transient eddy heat flux convergence-divergence dipole (Fig. 5b) sustains the cyclone-anticyclone pair balancing it by rising-subsiding motion with adiabatic cooling-warming of the atmosphere on that scale (not shown).

3.2. Mediterranean-East Asia bridge

The atmospheric feature related to severe and extreme wetness over the Tibetan Plateau is a more zonally elongated polar jet and a wave-like pattern that emerges from the core of the cross-Atlantic storm track and follows the subtropical westerly jet, which serves as a wave guide, towards the Tibetan Plateau and East Asia via the Mediterranean region (Fig. 6a). Note that the subtropical westerly jet is slightly weakened along 25°N , indicated by easterly anomalies (Fig. 6a).

Origin of the wave train is related to a more zonally oriented storm track extending well into western Europe (Fig. 6b), which provides a favourable condition for the wave activity fluxes to reach the northwest Europe and the Mediterranean region and to continue eastward therefrom. In contrast, in the case of severe and extreme dry events in the Tibetan Plateau, the North Atlantic storm track swings northeastward (Fig. 5b) and the excited wave activity

fluxes more often reach Scandinavia and travel towards the Tibetan Plateau via the 'great circle route' (Fig. 5a).

Associated with the Mediterranean-East Asia wave train, the Tibetan Plateau is under northerly wind anomalies (centered at 90°E), with southerly anomalies to its west (centered at 60°E) and westerly/easterly wind anomalies to its north/south, and is thus exposed to anticyclonic anomalies that tend to bring more moisture from the Arabian Sea towards the Tibetan Plateau, while the moisture supply from the Bay of Bengal may have reduced. Meanwhile, the western Pacific subtropical high extends westward inducing southerly wind anomalies in eastern China and northerly anomalies in the western North Pacific which, by generating anticyclonic anomalies, direct more moisture supply from the South China Sea and the western Pacific towards south China and the Tibetan Plateau. As a result, moisture convergence in the Tibetan Plateau is enhanced during the wet events (not shown, see Fig. 5b from Bothe et al., 2010).

It is important to stress that the composite anomaly of the stationary wave flux is of smaller amplitude between east of the Mediterranean region and the Tibetan Plateau and thus does not occur in Fig. 6a. However, this does not mean that the wave activity has disappeared in this region; on the contrary, it indicates that during severe and extreme wet events, the stationary wave activity does not differ from its climatological mean, which is rather strong in this region (Fig. 4), but wave activity fluxes occur more frequently and/or with stronger amplitude in the Mediterranean

region and downstream of the Tibetan Plateau. Both barotropic and baroclinic instability occur between east of the Mediterranean region and the Tibetan Plateau (not shown), and thus may contribute to the weakening of the wave flux anomalies, but neither provides a satisfactory answer, therefore requiring further investigation.

4. Conclusions and discussions

Two cross-Eurasia wave trains have been identified that influence the occurrence of severe and extreme dryness and wetness on the Tibetan Plateau by modulating the local atmospheric circulation. The wave activity fluxes generated in the North Atlantic storm track travel towards Asia via either the Scandinavia-Tibetan Plateau bridge or the Mediterranean-East Asia bridge, which closely corresponds to the different orientations and shifts of the North Atlantic storm track and the polar front jet.

During severe and extreme summer droughts on the Tibetan Plateau, the polar front jet swings northward, accompanied by the more southwest-northeast oriented North Atlantic storm track, which supports intense low pressure anomalies over Iceland and high pressure anomalies over Scandinavia and creates wave trains crossing Eurasia. On their southward 'great circle route', the wave trains, supported by changes in the local jets, modulate the flow around the Tibetan Plateau by generating cyclonic anomalies in north India and south China, which tend to direct the moisture supply from the Arabian Sea, the Bay of Bengal, and the South China Sea directly eastward towards the western Pacific thus reducing moisture transport into the Tibetan Plateau. Severe and extreme wetness events in the Tibetan Plateau are characterized by a more zonally oriented and elongated Atlantic storm track and atmospheric polar front jet stream. Wave trains emerging from the southern part of the storm track in the North Atlantic have now a higher chance to reach the Mediterranean region and subsequently propagate eastward along the subtropical westerly jet that serves as a wave guide. They interact with the Asian summer monsoon (ASM), enhancing the moisture convergence over the Tibetan Plateau with the moisture supply from the Arabian Sea and the South China Sea. These long-distance atmospheric bridges are composed of the storm track and wave train modules. They also provide the connection from the tropical Pacific to Europe via the North Pacific and the North Atlantic storm track (for the respective mechanisms, see [Fraedrich et al., 1993](#) and [Dréville et al., 2001](#)).

However, caution needs to be retained, as the composite study is based on six dry cases and eleven wet cases, which are far from sufficient to pinpoint a causal relationship between the switching of either of the wave trains and the set-up of the polar front jet. One disturbance more (or less) in one single month will suffice to change the monthly mean and may also change the composite picture as depicted in [Figs. 5 and 6](#). Therefore, on the one hand, the existence of such a close correspondence between the state of the polar front jet stream (and the North Atlantic storm track) and the cross-Eurasia wave trains is stressed. On the other hand, one has to be aware that the former should not be understood as a necessary or sufficient condition for the latter and vice versa, which may be derived with a larger group of samples.

Furthermore, in aiming to highlight the teleconnection routes of the upstream influence from the North Atlantic, the interpretation is constrained to manifesting the two atmospheric wave trains, and does not specifically discuss the oceanic influence on the Asian summer monsoon and the consequent effects on the moisture supply to the Tibetan Plateau. The ASM variability and its projection on the moisture transport are exposed to a global interaction network formed by various climate modes, including the active ENSO reflecting the tropical Pacific sea surface temperature (SST)

variability (e.g., [Webster and Yang, 1992](#); [Hong et al., 2008](#)), the Indian ocean warm pool (e.g., [Izumo et al., 2008](#); see review by [Schott et al., 2009](#)), and the tropical Atlantic SST variability (e.g., [Kucharski et al., 2007, 2008](#)). Moreover, other climate components also play active roles in interacting with the monsoon system, such as snow cover and ice sheets ([Gao et al., 2004](#); [Yin et al., 2007](#); [Severinghaus, 2009](#)).

Two wave trains described here may be considered as information channels, which transfer information of changes in the storm track and the atmospheric polar jet stream from the North Atlantic to the Tibetan Plateau and East Asia. These information channels may be switched on by anthropogenic processes. For instance, it has been observed that black carbon emitted from Southeast Asia and dust from North Africa induced a planetary-scale teleconnection spanning from North Africa through Eurasia to the North Pacific ([Kim et al., 2006](#)). Therefore, the topic of atmospheric bridging becomes even more challenging under global warming scenarios: questions like when and where the bridging processes are at work, how they transfer the information of climate variability, and above all, how the atmospheric bridges interact with local feedbacks, which is of primary importance for regional climate variability, still remain to be answered.

Acknowledgements

We would like to thank NOAA-CPC and the Model and Data group hosted at the Max Planck Institute for Meteorology for providing the data. We appreciate the guest editor's and two reviewers' interest; their suggestions and comments have helped shaping this manuscript.

Appendix: Standardized Precipitation Index (SPI)

As monthly precipitation differs strongly in various regions on the Tibetan Plateau, the present study adopts the Standardized Precipitation Index (SPI; [McKee et al., 1993](#)), which establishes reasonable agreement of point-wise and plateau-averaged drought and wetness classifications.

The transformation depends critically on the assumed statistical distribution of monthly precipitation. A false distribution type may lead to systematic errors, most pronounced for the extreme cases. The commonly used gamma distribution ([Bordi et al., 2007](#)) does not necessarily hold for all months or all regions considered; better fits can be achieved using the Weibull distribution. In order to still use a single unifying distribution type, the 'Generalised Gamma Distribution' is applied instead, employing a re-parameterized version (for details, see [Sienz et al., 2007](#)). The SPI can be constructed for different timescales characterizing periods of meteorological (months), agricultural (season) and hydrological (year) dryness or wetness. In this article, the monthly timescale is considered as a lower bound for dry and wet spells and their extremes ([Dracup et al., 1980](#)). The SPI classification following [McKee et al. \(1993\)](#) is shown in [Table 1](#).

Table 1

Classification of Standardized Precipitation Index (SPI) and probability (%) of events.

SPI intervals	SPI classes	p value
$SPI \geq 2$	Extremely wet	2.3
$2 > SPI \geq 1.5$	Severely wet	4.4
$1.5 > SPI \geq 1$	Moderately wet	9.2
$1 > SPI \geq -1$	Normal	68.2
$-1 > SPI \geq -1.5$	Moderately dry	9.2
$-1.5 > SPI \geq -2$	Severely dry	4.4
$SPI \leq -2$	Extremely dry	2.3

References

- Ambrizzi, T., Hoskins, B.J., Hsu, H.-H., 1995. Rossby wave propagation and teleconnection patterns in the austral winter. *Journal of Atmospheric Sciences* 52, 3661–3672.
- An, Z., Kutzbach, J.E., Prell, W.E., Porter, S.C., 2001. Evolution of Asian monsoons and phased uplift of the Himalaya-Tibetan Plateau since late Miocene times. *Nature* 411, 62–66.
- Beck, C., Grieser, J., Rudolf, B., 2005. A New Monthly Precipitation Climatology for the Global Land Areas for the Period 1951 to 2000. Climate Status Report No. 2004. German Weather Service, Offenbach, pp. 181–190.
- Bordi, I., Fraedrich, K., Petitta, M., Suter, A., 2007. Extreme value analysis of wet and dry periods in Sicily. *Theoretical and Applied Climatology* 87, 61–71. doi:10.1007/s00704-005-0195-3.
- Bordi, I., Suter, A., 2001. Fifty years of precipitation: some spatially remote teleconnections. *Water Resources Management* 15, 247–280.
- Bothe, O., Fraedrich, K., Zhu, X., 2010. The large-scale circulations and summer drought and wetness on the Tibetan plateau. *International Journal of Climatology* 30, 844–855.
- Branstator, G., 2002. Circumglobal teleconnections, the jet stream waveguide, and the North Atlantic Oscillation. *Journal of Climate* 15, 1893–1910.
- Ding, Q., Wang, B., 2005. Circumglobal teleconnection in the northern hemisphere summer. *Journal of Climate* 18, 3483–3505.
- Dracup, J.A., Lee, K.S., Paulson, E.G., 1980. On the definition of droughts. *Water Resources Research* 16, 297–302.
- Drévillion, M., Terray, L., Rogel, P., Cassou, C., 2001. Mid latitude Atlantic SST influence on European winter climate variability in the NCEP reanalysis. *Climate Dynamics* 18, 331–344.
- Fekete, B.M., Vörösmarty, C.J., Grabs, W., 1999. Global Composite Runoff Fields Based on Observed River Discharge and Simulated Water Balances. Technical Report No. 22. Global Runoff Data Center, Koblenz, 115.
- Fekete, B.M., Vörösmarty, C.J., Grabs, W., 2000. UNH/GRDC Composite Runoff Fields V 1.0. See. Global Runoff Data Center (GRDC), Durham, NH. <http://www.grdc.sr.unh.edu/> Complex Systems Research Center, University of New Hampshire, Koblenz, Germany.
- Feng, S., Hu, Q., 2008. How the North Atlantic Multidecadal Oscillation may have influenced the Indian summer monsoon during the past two millennia. *Geophysical Research Letters* 35, L01707. doi:10.1029/2007GL032484.
- Flohn, H., 1964. Investigations on the tropical easterly jet. *Bonner Meteorologische Abhandlungen* 4, 1–83.
- Flohn, H., 1968. Contributions to a Meteorology of the Tibetan Highlands. Atmospheric Science Paper No. 130. Department of Atmosphere Science, Colorado State University, Colorado.
- Fraedrich, K., Banzer, C., Burkhardt, U., 1993. Winter climate anomalies in Europe and their associated circulation at 500 hPa. *Climate Dynamics* 8, 161–175.
- Gao, R., Wei, Z., Dong, W., Zhong, H., 2004. Impact of the anomalous thawing in the Tibetan Plateau on summer precipitation in China and its mechanism. *Advances in Atmospheric Sciences* 22 (2), 238–245.
- Goswami, B.N., Madhusoodanan, M.S., Neema, C.P., Sengupta, D., 2006. A physical mechanism for North Atlantic SST influence on the Indian summer monsoon. *Geophysical Research Letters* 33, L02706. doi:10.1029/2005GL024803.
- Gupta, A.K., Anderson, D.M., Overpeck, J.T., 2003. Abrupt changes in the Asian southwest monsoon during the Holocene and their links to the North Atlantic Ocean. *Nature* 421, 354–357.
- Hong, C.-C., Lu, M.-M., Kanamitsu, M., 2008. Temporal and spatial characteristics of positive and negative Indian Ocean dipole with and without ENSO. *Journal of Geophysical Research* 113, D08107. doi:10.1029/2007JD009151.
- Hoskins, B.J., Ambrizzi, T., 1993. Rossby wave propagation on a realistic longitudinally varying flow. *Journal of the Atmospheric Sciences* 50, 1661–1671.
- Izumo, T., Montégut, C.D., Luo, J.-J., Behera, S.K., Masson, S., Yamagata, T., 2008. The role of the western Arabian Sea upwelling in Indian monsoon rainfall variability. *Journal of Climate* 21, 5603–5623.
- Kim, M.-K., Lau, W.K.M., Chin, M., Kim, K.-M., Sud, Y.C., Walker, G.K., 2006. Atmospheric teleconnection over Eurasia induced by aerosol radiative forcing during boreal spring. *Journal of Climate* 19, 4700–4717.
- Kucharski, F., Bracco, A., Yoo, J.H., Molteni, F., 2007. Low-frequency variability of Indian monsoon-ENSO relationship and the tropical Atlantic: the “weakening” of the 1980s and 1990s. *Journal of Climate* 20, 4255–4266.
- Kucharski, F., Bracco, A., Yoo, J.H., Molteni, F., 2008. Atlantic forced component of the Indian monsoon interannual variability. *Geophysical Research Letters* 35, L04706. doi:10.1029/2007GL033037.
- Li, J., Yu, R., Zhou, T., 2008. Teleconnection between NAO and climate downstream of the Tibetan Plateau. *Journal of Climate* 21, 4680–4690.
- Liu, X., Yin, Z.-Y., 2001. Spatial and temporal variation of summer precipitation over the eastern Tibetan Plateau and the North Atlantic Oscillation. *Journal of Climate* 14, 2896–2909.
- McKee, T.B., Doeskin, N.J., Kleist, J., 1993. The Relationship of Drought Frequency and Duration to Time Scales. 8th Conference on Applied Climatology. American Meteorological Society, Anaheim, pp. 179–184.
- d’Orgeville, M., Peltier, W.R., 2007. On the Pacific Decadal oscillation and the Atlantic multidecadal oscillation: might they be related? *Geophysical Research Letters* 34, L23705. doi:10.1029/2007GL031584.
- Schott, F., Xie, S.-P., McCreary, J.P., 2009. Indian Ocean circulation and climate variability. *Reviews of Geophysics* 47, RG1002. doi:10.1029/2007RG000245.
- Severinghaus, J.P., 2009. Monsoons and melt-downs. *Science* 326, 240–241.
- Sienz, F., Bordi, I., Fraedrich, K., Schneidereit, A., 2007. Extreme dry and wet events in Iceland: observations, simulations and scenarios. *Meteorologische Zeitschrift* 16, 9–16.
- Uppala, S.M., Kallberg, P.W., Simmons, A.J., Andrae, U., Bechtold, V.D., Fiorino, M., Gibson, J.K., Haseler, J., Hernandez, A., Kelly, G.A., Li, X., Onogi, K., Saarinen, S., Sokka, N., Allan, R.P., Andersson, E., Arpe, K., Balmaseda, M.A., Beljaars, A.C.M., Van De Berg, L., Bidlot, J., Bormann, N., Caires, S., Chevallier, F., Dethof, A., Dragosavac, M., Fisher, M., Fuentes, M., Hagemann, S., Holm, E., Hoskins, B.J., Isaksen, I., Janssen, P.A.E.M., Jenne, R., McNally, A.P., Mahfouf, J.F., Morcrette, J.J., Rayner, N.A., Saunders, R.W., Simon, P., Sterl, A., Trenberth, K.E., Untch, A., Vasiljevic, D., Viterbo, P., Woollen, J., 2005. The ERA-40 re-analysis. *Quarterly Journal of the Royal Meteorological Society* 131, 2961–3012. doi:10.1256/qj.04.176.
- Wang, B., Bao, Q., Hoskins, B.J., Wu, G., Liu, Y., 2008. Tibetan Plateau warming and precipitation changes in East Asia. *Geophysical Research Letters* 35, L14702. doi:10.1029/2008GL034330.
- Webster, P.J., Yang, S., 1992. Monsoon and ENSO: selectively interactive systems. *Quarterly Journal of the Royal Meteorological Society* 118, 877–926.
- Yang, S., Lau, K.-M., Yoo, S.-H., Kinter, J.L., Miyakoda, K., 2004. Upstream subtropical signals preceding the Asian summer monsoon circulation. *Journal of Climate* 17, 4213–4229.
- Ye, H., 2000. Decadal variability of Russian winter snow accumulation and its associations with Atlantic sea surface temperature anomalies. *International Journal of Climatology* 20, 1709–1728.
- Yin, Q.Z., Berger, A., Driesschaert, E., Goosse, H., Loutre, M.F., Crucifix, M., 2007. Modelling a strong East Asian summer monsoon in a globally cool Earth, the MIS-13 case. *Climate of the Past Discussions* 3, 1261–1282.
- Zhang, R., Delworth, T.L., 2006. Impact of Atlantic multidecadal oscillations on India/Sahel rainfall and Atlantic hurricanes. *Geophysical Research Letters* 33, L17712. doi:10.1029/2006GL026267.
- Zhang, R., Delworth, T.L., 2007. Impact of the Atlantic multidecadal oscillation on north Pacific climate variability. *Geophysical Research Letters* 34, L23708. doi:10.1029/2007GL031601.